Efficacy of Nivolumab in Pediatric Cancers with High Mutation Burden and Mismatch Repair Deficiency

Anirban Das[1], Uri Tabori[1], Lauren C. Sambira Nahum[1], Natalie B. Collins[2], Rebecca Deyell[3], Rina Dvir[4], Cecile Faure-Conter[5], Timothy E. Hassall[6], Jane E. Minturn[7], Melissa Edwards[1], Elissa Brookes[1], Vanessa Bianchi[1], Adrian Levine[1], Simone C. Stone[8], Sumedha Sudhaman[1], Santiago Sanchez Ramirez[1], Ayse B. Ercan[1], Lucie Stengs[1], Jill Chung[1], Logine Negm[1], Gad Getz[9], Yosef E. Maruvka[10], Birgit Ertl-Wagner[1], Pamela S. Ohashi[8], Trevor Pugh[8], Cynthia Hawkins[1], Eric Bouffet[1], and Daniel A. Morgenstern[1]

ABSTRACT

Purpose: Checkpoint inhibitors have limited efficacy for children with unselected solid and brain tumors. We report the first prospective pediatric trial (NCT02992964) using nivolumab exclusively for refractory nonhematologic cancers harboring tumor mutation burden (TMB) ≥5 mutations/megabase (mut/Mb) and/or mismatch repair deficiency (MMRD).

Patients and Methods: Twenty patients were screened, and 10 were ultimately included in the response cohort of whom nine had TMB >10 mut/Mb (three initially eligible based on MMRD) and one patient had TMB between 5 and 10 mut/Mb.

Results: Delayed immune responses contributed to best overall response of 50%, improving on initial objective responses (20%) and leading to 2-year overall survival (OS) of 50% [95% confidence interval (CI), 27–93]. Four children, including three with refractory malignant gliomas are in complete remission at a median follow-up of 37 months (range, 32.4–60), culminating in 2-year OS of 43% (95% CI, 18.2–100). Biomarker analyses confirmed benefit in children with germline MMRD, microsatellite instability, higher activated and lower regulatory circulating T cells. Stochastic mutation accumulation driven by underlying germline MMRD impacted the tumor microenvironment, contributing to delayed responses. No benefit was observed in the single patient with an MMR-proficient tumor and TMB 7.4 mut/Mb.

Conclusions: Nivolumab resulted in durable responses and prolonged survival for the first time in a pediatric trial of refractory hypermutated cancers including malignant gliomas. Novel biomarkers identified here need to be translated rapidly to clinical care to identify children who can benefit from checkpoint inhibitors, including upfront management of cancer.

See related commentary by Mardis, p. 4701

Introduction

Immune checkpoint inhibition (ICI) targeting programmed-death 1 (PD1) and its ligand (PD-L1) has shown improved survival in adults with advanced cancers (1–4). The best responses have been observed in cancers exhibiting high tumor mutation burden (TMB), mismatch repair deficiency (MMRD), microsatellite instability (MSI), or PD-L1 expression (3–5). Notably, hypermutant gliomas have failed to respond due to the immune privilege of the central nervous system (CNS), their immunosuppressive microenvironment (6), and the subclonal nature of MMRD in these cancers (7–9).

Previous clinical trials in children using anti-PD1 [nivolumab (10), pembrolizumab (11)], anti–PD-L1 [atezolizumab (12), avelumab (13)], and anti-CTLA4 [ipilimumab (14)] have shown limited efficacy restricted to lymphomas and rare solid tumors. In addition to low TMB and immunogenicity contributing to an "immune-cold" microenvironment (11), this has been attributed to low expression of MHC (15), an immature immune system (16) and gut microbiome (17), and the presence of an immunosuppressive microenvironment enriched for macrophages (18). The failure of ICI in unselected pediatric cancers has led to recommendations of avoiding ICI monotherapy trials in children without robust biological rationale (19, 20).

The improved outcomes using ICI in refractory MMRD cancers in adults (21) and detection of hypermutation in 5% of pediatric cancers (22), the majority of which were driven by MMRD, prompted us to hypothesize that such a molecularly selected cohort of cancers in children may respond to ICI monotherapy. Hence, we developed NCT02992964, an investigator-initiated, multicenter, open-label, single-arm pilot study in which pediatric patients with relapsed/refractory cancers with increased TMB and/or MMRD were treated with nivolumab. The trial included an initial "Part 1: Molecular Profiling," allowing patients to consent to analyses to confirm eligibility. This required the presence of a mutation in MMR genes (*MLH1, MSH2, MSH6, PMS2, EPCAM, MSH3*) or a loss of MMR protein expression on IHC, hypermutation, or a corresponding mutational signature (COSMIC; ref. 23) on sequencing, MSI, a history of germline conditions linked to hypermutation (constitutional mismatch repair deficiency syndrome/CMMRD, Lynch syndrome,

[1]Hospital for Sick Children and Department of Paediatrics, University of Toronto, Toronto, Ontario. [2]Dana-Farber/Boston Children's Cancer and Blood Disorders Center, Boston, Massachusetts. [3]BC Children's Hospital, Vancouver, British Columbia. [4]Tel Aviv Sourasky Medical Center, Tel Aviv, Israel. [5]Centre Léon Bérard, Lyon, France. [6]Queensland Children's Hospital, Brisbane, Australia. [7]Children's Hospital of Philadelphia, Philadelphia, Pennsylvania. [8]Princess Margaret Cancer Centre and University of Toronto, Toronto, Ontario. [9]Broad Institute of Harvard and MIT, Cambridge, Massachusetts. [10]Technion- Israel Institute of Technology, Tel-Aviv, Israel.

Corresponding Authors: Daniel A. Morgenstern, The Hospital for Sick Children, University of Toronto, 555 University Avenue, Toronto, ON M5G 1X8, Canada. E-mail: daniel.morgenstern@sickkids.ca; Eric Bouffet, eric.bouffet@sickkids.ca; and Uri Tabori, uri.tabori@sickkids.ca

Clin Cancer Res 2023;29:4770–83

doi: 10.1158/1078-0432.CCR-23-0411

Translational Relevance

This trial represents the first prospective assessment of the utility of immune checkpoint blockade in pediatric cancers with increased mutation burden and/or mismatch repair deficiency. The best overall response rate of 50% and remarkable prolonged overall survival particularly in patients with relapsed high-grade glioma demonstrates a clear role for immune checkpoint inhibition (ICI) in this rare pediatric population and lays a foundation for incorporating ICI in the upfront treatment of these patients.

xeroderma pigmentosum), or prior treatment with temozolomide. Patients were eligible for "Part 2: Treatment and Companion Biomarker Studies" provided they separately consented for therapy, had a measurable or evaluable relapsed/refractory cancer with no alternative treatment, and confirmation of MMRD and/or hypermutation.

Herein, we report the unique antitumor responses and survival benefit using nivolumab observed in NCT02992964 for children with advanced, nonhematologic malignancies with elevated mutation burden and/or MMRD. We also present the results of exploratory analyses that suggest that definite genomic and immune biomarkers can help identify children whose cancers can benefit from ICI monotherapy.

Patients and Methods

Trial design and treatment

NCT02992964 was an investigator-initiated, multicenter, open-label, single-arm pilot study in which pediatric patients ages ≥12 months and <25 years of age with relapsed/refractory cancers with elevated TMB and/or MMRD were treated with nivolumab 3 mg/kg every 2 weeks until confirmed disease progression, intolerable toxicity, or for a maximum of 24 months. The study was approved by Institutional Ethics Review Boards and competent authorities in each center, and conducted in accordance with International Ethical Guidelines for Biomedical Research Involving Human Subjects (CIOMS). Written informed consent was obtained from all patients or parents/guardians according to local regulations. Nivolumab and funding to support the conduct of the study was provided by Bristol Myers Squibb.

Patients

The protocol included an initial "Part 1: Molecular Profiling" option allowing patients to consent to sequencing to confirm eligibility. This required, either in the recurrent or primary tumor, the presence of a mutation in MMR genes (*MLH1, MSH2, MSH6, PMS2, EPCAM, MSH3*) or loss of protein expression on IHC, hypermutation or a corresponding mutational signature (COSMIC; ref. 23) on sequencing performed locally, MSI, a history of germline conditions linked to hypermutation (CMMRD, Lynch syndrome, xeroderma pigmentosum), or prior treatment with temozolomide.

Patients were eligible for "Part 2: Treatment and Companion Biomarker Studies" provided they separately consented for therapy, had a relapsed/refractory cancer for which there was no known curative therapy, or therapy proven to prolong survival with an acceptable quality of life, baseline imaging within 14 days of starting treatment with measurable or evaluable disease, and confirmation of MMRD and/or TMB ≥5 mutations/megabase (mut/Mb). The latter was determined by measurement of TMB either via FoundationOne (Foundation Medicine), or an equivalent next-generation sequencing cancer-gene panel. Patients with a TMB ≥5 mut/Mb were eligible, with separate cohorts for TMB 5 to 10 mut/Mb and >10 mut/Mb. Patients with a history of autoimmune diseases, human immunodeficiency virus, chronic hepatitis B/C, prior allogeneic or solid organ transplant or ICI treatment, uncontrolled infection or requiring corticosteroid therapy at greater than physiologic doses were excluded.

Study assessments and endpoints

Disease status was monitored every 2 months while on therapy, and the response was evaluated using different criteria based on the type of tumor: iRECIST (Immunotherapy Response Evaluation Criteria in Solid Tumours) for solid tumors, revised INRC (International Neuroblastoma Response Criteria) for neuroblastoma, and iRANO (Immunotherapy Response Assessment in Neuro-Oncology) for CNS malignancies. The response was labeled as complete remission (CR), partial remission (PR), or progressive disease (PD) based on the assessment. The primary objective was to evaluate objective response rate (ORR = CR + PR). For correctly assigning immune responses following possible pseudoprogression, clinically stable patients could continue therapy beyond initial unconfirmed progression (iUPD), with subsequent scans being used to establish confirmed progression, or delayed "immune" CR or PR, which could then be included in the best overall response (iBOR). iBOR was defined as the best response recorded from the start of the treatment until disease progression/recurrence), even after discontinuation of protocol therapy (refs. 24, 25, 27, 28; details in Supplementary Tables S5–S9 of trial protocol: Supplementary Appendix). It was mandatory for all patients who demonstrated CR, PR, or stable disease (SD) lasting beyond six cycles to have a central review of the radiology at the Hospital for Sick Children. If feasible, histologic evaluation was allowed to resolve ambiguity regarding immune responses.

Secondary objectives included determination of progression-free survival (PFS), overall survival (OS), and evaluating the safety and toxicity of treatment. PFS was defined from time of first study medication dose to first progression that either involved significant clinical deterioration and/or was unambiguously confirmed radiologically as PD. OS was defined as time from the first study medication to death. Adverse events were graded according to the NCI's Common Terminology Criteria for Adverse Events v.4.03.

Biomarker analyses

Exploratory biomarker analyses included whole-exome sequencing (WES) and analyses of total and microsatellite in(sertion)-del(etions) (MSI) burden, plus IHC for CD8 and PD-L1 expression, and peripheral blood immune profiling using flow cytometry, and T-cell receptor (TCR) rearrangement using methods previously published by our group (29). All bioinformatics analyses were performed on the SickKids High Performance Cluster (HPF) and the University Health Network (UHN) High Performance Cluster for Health (H4H). The details are provided below.

For WES, genomic DNA, along with matched germline blood samples for available cases was extracted using the PaxGene Blood DNA Extraction Kit (catalog No./ID: 761133) for blood samples, Qiagen DNeasy Blood & Tissue Kits (catalog No./ID: 69504) for frozen tissue, and MasterPure Complete DNA and RNA Purification Kit (Epicentre #MC85200) for paraffin-embedded tissue. WES was performed at The Centre for Applied Genomics, SickKids, using SureSelect Agilent All Exon v5 kit, followed by sequencing (150X) on Illumina HiSeq 2500. The software bcl2fastq2 v2.17 was used to

generate raw fastq files. Alignment to the hg38 reference genome, followed by preprocessing and QC was adapted from the GATK standard pipeline, using BWA-MEM 0.7.12 (alignment), BAMQC, Picard 2.6.0 (QC). Somatic variant calling was done post alignment, using processed bam files from tumor and matched normal samples, to call both single-nucleotide variants (SNV) and insertion deletion (indel) variants. A consensus vcf file of shared variants across two or more of four variant callers (Mutect v1.1.5, GATK v3.6/Mutect2, Strelka v1.0.14, and Varscan2 Somatic v2.4.2) was generated for SNV and indels separately, using VCFtools 0.1.15, and these vcfs were annotated using VEP v83. We used the built-in algorithms in the GATK mutect2 pipeline sequence to correct for context-dependent artifacts related to tissue source and processing by using the read-orientation bias filter and excluding low allele fraction SNP where evidence for the alternate allele consists almost entirely of F1R2 reads or F2R1 reads. The TMB (SNV per megabase) from WES data was calculated by counting the total number of somatic SNV divided by the total number of callable bases in megabases (∼50 Mb). DeconstructSigs (30) was used to determine COSMIC signatures (23, 31) in the mutation spectrum within a trinucleotide context for each sample.

Microsatellite (MS) indels were called on the bam files of tumor and matched normal samples, using an in-house pipeline using MSMuTect. The detailed methods for this algorithm have been reported previously (32, 33). Briefly, repeats of five or more nucleotides were considered to be MS loci, and using the PHOBOS algorithm and the lobSTR approach, tumor and normal BAM files were aligned with their 5′ and 3′ flanking sequences. Each MS-locus allele was estimated using the empirical noise model, which is the probability of observing a read with a MS length k and motif m, where the true length of the allele is j with the motif m. This was used to call the MS alleles with the highest likelihood of being the true allele at each MS-locus. The alleles of microsatellite (MS) markers for each tumor and its matched normal sample were determined separately. These alleles were then compared to identify the mutations present at the MS loci in the tumor samples. The Akaike Information Criterion score was assigned to both the tumor and normal models, and a threshold score that was determined by using simulated data was applied to make the final MS-indel call.

For IHC analysis of the immune microenvironment, 4-μm-thick sections of formalin-fixed paraffin-embedded surgical specimens were stained using an automated stainer (Dako OMNIS) with the following primary antibodies: PD-L1 (clone28-8, Abcam, 1/500) and CD8 (Clone c8/144B, Dako OMINS). Measurements were recorded as the number of positive cells per tissue surface unit in square millimetres. Quantitative evaluation of the IHC stains was performed by examine each section using at least five to seven different high-power fields with the most abundant tumor-infiltrating lymphocyte areas.

For TCR rearrangement repertoire profiling, genomic DNA was extracted (methods as above) from tumors. These were transferred to the Pugh laboratory at the UHN in Toronto, where library preparation and capTCRseq (34) hybrid capture were performed. Following library preparation, the samples were sequenced first on a MiSeq for QC purposes and then 300 ng of each sample, pooled in a ratio of 1:1:1, was processed for a three-step capture using target hybrid capture panel (8). Postcapture QC was performed on a MiSeq, followed by sequencing of up to a depth of approximately 2 million reads on the NextSeq. Postsequencing, the raw data were analyzed using MiXCR version 2.1.12, "iNext," "immunarch" R packages and Pugh Lab customized functions on R version 3.5 to look at TCR rearrangements in the form of unique clonotypes (VDJ rearranged sequences) for TCRs alpha, beta, gamma, and delta. As the total read depth varied across the cohort, affecting the total successfully aligned reads, all raw fastq reads were downsampled to approximately 1 million reads. QC parameters of percent aligned reads, reads used in clonotypes, final clonotype count, and the total number of clonotypes per 1,000 reads were considered.

For flow cytometry analysis, viable frozen peripheral blood mononuclear cells were incubated with Fc block (BD Biosciences) prior to staining for surface markers (anti-CD3 - clone UCHT1, anti-CD4 – clone RPA-T4, anti-CD8 – clone RPA-T8, anti-4-1BB– clone 4B4-1, anti-TIGIT – clone MBSA43, anti-Ki67 – clone 20Raj1) and viability dye (eBioscience). Cells were fixed and permeabilized for intercellular staining with the Foxp3 transcription factor staining buffer set (BD). Flow cytometry voltages were set using Rainbow beads (Spherotech) with the same setting between experiments. Samples were acquired on a BD LSR Fortessa flow cytometer, and data were analyzed using the FlowJo software.

Statistical analyses

The trial was originally planned as a pilot study for which the initial aim was to accrue 20 pediatric patients with CMMRD. Following encouraging results in adult trials for hypermutant cancers, an amendment was made, and the study inclusion criteria was expanded to include patients with tumors harboring high TMB, as well as those with CMMRD, and consequently the total enrollment was increased to 50 patients. We planned to recruit patients into two cohorts of TMB 5 to 10 (cohort A) and ≥10 mut/Mb (cohort B) using a Simon two-stage optimal design within each cohort. Cohort A was designed with power of 85% and one-sided alpha of 0.05 to test a true response rate of 35% again a null hypothesis ORR of 10%. If there were ≥2 responders within the first 10 patients, the cohort would expand to 21 patients, and the outcome would be positive if there were ≥5 responses. Cohort B was designed with a power of 80% and one-sided alpha of 0.05 to test a true response rate of 30% againt a null hypothesis ORR of 10%. If there were ≥2 responders within the first 10 patients, the cohort would expand to

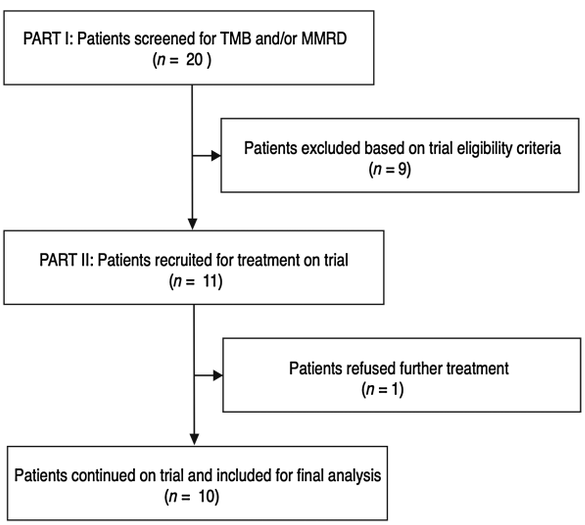

Figure 1.
CONSORT diagram showing flow of patients.

Table 1. Summary of the demographics, clinical features, biomarkers, treatment details, and outcomes of patients treated on NCT02992964 ($n = 10$).

ID	Age (y)	Sex	Genetic predisposition	Race	Cancer diagnosis	MMR Immuno-histochemistry	TMB (mut/Mb)	Total indels	MS indels	*POLE/POLD1* variants	COSMIC SBS v.2	Baseline CD8 expression	Baseline PD-L1 expression	Pretrial palliative radiation	Objective response on trial (Criteria)	Best overall response	Nivolumab posttrial termination	Other nonimmune systemic therapies	OS (mo)	Status
P1	13	F	Lynch syndrome	Caucasian	Anaplastic astrocytoma	PMS2, MLH1 lost in tumor only	14.3	595	1,588	Absent	1, 15	7%	Faint	No	Progressive disease (iRANO)	Progressive disease	No	None	1.8	Dead
P2	17	F	Lynch syndrome	Caucasian	Colorectal carcinoma	MSH2, MSH6 lost in tumor only	25.4	892	704	Absent	21, 30	2.70%	Faint	No	Stable disease (RECIST)	Pathological complete remission	No	None	53.12	Alive
P3	12	F	Lynch syndrome	Caucasian	Glioblastoma	MSH2, MSH6 lost in tumor only	15.9	434	892	Absent	1, 6, 18	0%	Absent	No	Stable disease (iRANO)	Delayed partial response	Yes	After 12 months: Nilotinib, Everolimus	15.85	Dead
P4	15	M	Lynch syndrome	Caucasian	Glioblastoma	MSH2, MSH6 lost in tumor only	253.64	801	509	*POLE; p.S459F*	1, 5, 12, 20	2%	>1%	No	Complete response (iRANO)	Complete response	No	None	35.14	Alive
P5	16	F	Germline *PALB2*	Caucasian	Neuro-blastoma	All MMR stains retained	11.35	X	X	Absent	3, 8, 12, 18	X	X	No	Stable disease (Revised INRC)	Stable disease	No	MIBG, PARP-inhibitors	31.29	Dead
P6	13	M	CMMRD	Asian	Glioblastoma	PMS2 lost in both tumor and germline	714.46	1,091	1291	*POLE; p.S461P*	1, 14, 15	7.30%	>1%	No	Partial response (iRANO)	Partial response	Yes	None	26.56	Alive
P7	9	F	CMMRD	Native American	Glioblastoma	PMS2 lost in both tumor and germline	581.84	903	989	*POLE; p.S459F*	1, 10, 14, 15	0.60%	Absent	No	Stable disease (iRANO)	Delayed complete response	Yes	None	25.45	Alive
P8	14	M	None	Caucasian	Anaplastic astrocytoma	Focal, heterogeneous MSH6 loss	106.42	68	19	Absent	11	>10%	>1%	No	Progressive disease (iRANO)	Progressive disease	No	None	7.2	Dead
P9	18	M	Lynch syndrome	African American	Glioblastoma	MSH2, MSH6 lost in tumor only	33.46	133	185	Absent	1, 15	0.70%	Absent	No	Stable disease (iRANO)	Stable disease	Yes	None	16.24	Dead
P10	11	M	Li-Fraumeni syndrome	Hispanic	Adrenocortical carcinoma	All MMR stains retained	7.4	14	29	Absent	4, 23, 29	X	X	No	Progressive disease (iRECIST)	Progressive disease	None	None	0.72	Dead

Abbreviations: CMMRD, constitutional MMR deficiency; F, female; M, male; MIBG, iodine meta-iodobenzylguanidine; MMR, mismatch repair; MS, microsatellite; mut/Mb, mutations/megabase; PARP, poly (ADP-ribose) polymerase; SBS, single-base substitution signatures; X, data not available; y, years.

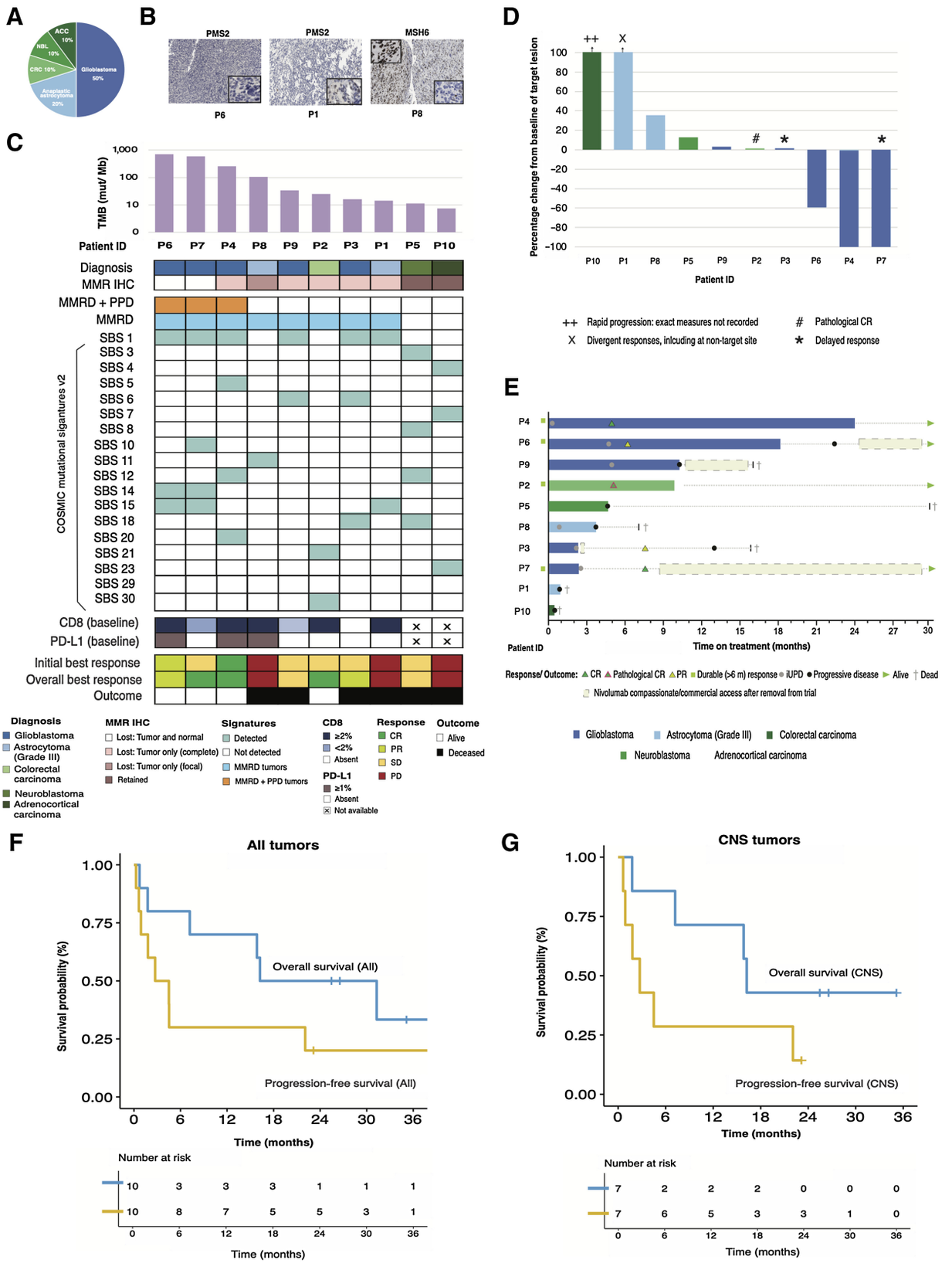
A
ACC 10%
NBL 10%
CRC 10%
Glioblastoma 50%
Anaplastic astrocytoma 20%
B
PMS2
PMS2
MSH6
P6
P1
P8
C
TMB (mut/ Mb)
1,000
100
10
0
Patient ID
P6 P7 P4 P8 P9 P2 P3 P1 P5 P10
Diagnosis
MMR IHC
MMRD + PPD
MMRD
COSMIC mutational signatures v2
SBS 1
SBS 3
SBS 4
SBS 5
SBS 6
SBS 7
SBS 8
SBS 10
SBS 11
SBS 12
SBS 14
SBS 15
SBS 18
SBS 20
SBS 21
SBS 23
SBS 29
SBS 30
CD8 (baseline)
PD-L1 (baseline)
Initial best response
Overall best response
Outcome
Diagnosis
Glioblastoma
Astrocytoma (Grade III)
Colorectal carcinoma
Neuroblastoma
Adrenocortical carcinoma
MMR IHC
Lost: Tumor and normal
Lost: Tumor only (complete)
Lost: Tumor only (focal)
Retained
Signatures
Detected
Not detected
MMRD tumors
MMRD + PPD tumors
CD8
≥2%
<2%
Absent
PD-L1
≥1%
Absent
Not available
Response
CR
PR
SD
PD
Outcome
Alive
Deceased
D
Percentage change from baseline of target lesion
100
80
60
40
20
0
−20
−40
−60
−80
−100
++
X
#
*
*
P10 P1 P8 P5 P9 P2 P3 P6 P4 P7
Patient ID
++ Rapid progression: exact measures not recorded
X Divergent responses, inlcuding at non-target site
Pathological CR
* Delayed response
E
P4
P6
P9
P2
P5
P8
P3
P7
P1
P10
0 3 6 9 12 15 18 21 24 27 30
Patient ID
Time on treatment (months)
Response/ Outcome: CR Pathological CR PR Durable (>6 m) response iUPD Progressive disease Alive Dead
Nivolumab compassionate/commercial access after removal from trial
Glioblastoma
Astrocytoma (Grade III)
Colorectal carcinoma
Neuroblastoma
Adrenocortical carcinoma
F
All tumors
Survival probability (%)
1.00
0.75
0.50
0.25
0.00
Overall survival (All)
Progression-free survival (All)
0 6 12 18 24 30 36
Time (months)
Number at risk
10 3 3 3 1 1 1
10 8 7 5 5 3 1
0 6 12 18 24 30 36
Time (months)
G
CNS tumors
Survival probability (%)
1.00
0.75
0.50
0.25
0.00
Overall survival (CNS)
Progression-free survival (CNS)
0 6 12 18 24 30 36
Time (months)
Number at risk
7 2 2 2 0 0 0
7 6 5 3 3 1 0
0 6 12 18 24 30 36
Time (months)

Table 2. Treatment-related adverse events that were considered possibly, probably, or definitely related to study therapy for children treated on NCT02992964 ($n = 11$).

	Number of patients		
Adverse event	**All grades**	**Grade 3**	**Grade 4**
Headache	3	1	0
Fatigue	3	0	0
Hydrocephalus	1	0	1
Papilledema	1	0	0
Other neurologic[a]	2	0	0
Lipase increased	1	1	1
Pancreatitis	1	1	0
Other gastrointestinal[b]	3	0	0
Other skin[c]	2	0	0
Other[d]	3	0	0
Lymphopenia	1	1	0
Other laboratory[e]	1	0	0

[a]Gait disturbance, dizziness, tremor, seizure.
[b]Vomiting, nausea, diarrhea, blood in stool, gastritis.
[c]Alopecia, dry skin.
[d]Dyspnea, flu-like symptoms, noninfective cystitis, arthralgia.
[e]Alanine aminotransferase increased, hypokalemia, hyponatremia, anemia.

29 patients, and the outcome would be positive if there were ≥6 responses. Unfortunately, the study was terminated prematurely due to slow recruitment and loss of funding. As per predefined protocol criteria, patients exhibiting objective disease progression prior to the end of cycle 1 were considered evaluable for response. For all other patients, only those who have measurable disease present at baseline, had received at least one cycle of therapy (two doses of nivolumab) and had their disease reevaluated were considered evaluable for response. All enrolled patients who had received at least one dose of nivolumab were evaluable for the safety data. Patients who were removed from protocol therapy continued to have the required follow-up observations and documentation of additional treatments received, with the only exception for this continued documentation being the patient's withdrawal of consent, in which case only data collected prior to the withdrawal of consent could be evaluated.

PFS and OS for treated patients were estimated using the Kaplan–Meier method with patients censored, as necessary, at date of last follow-up. For correlative biomarker analyses, best overall response (iBOR) was used as a manifestation of true immune, including delayed, responses. For the serial immune correlates, landmark analysis was performed at 3 and 6 months. Furthermore, as these correlates changed over time, we performed time-dependent covariate analysis using a modified Cox model as described previously (https://cran.r-project.org/web/packages/survival/vignettes/timedep.pdf). All statistical analyses were performed with R v.4.2.1. All P values were two sided, with a cutoff of 0.05 for significance. Adjustments to the P values for multiple comparisons to control for FDR were performed using methods as previously reported by Benjamini and colleagues (35, 36). Plots were edited for aesthetics using Adobe Illustrator v.23.0.1.

Data availability

All data relevant to this work are available in European Genome Phenome Archive under accession number EGAS00001007393 (https://ega-archive.org/studies/EGAS00001007393) and accessible through communication with the corresponding authors. All codes are publicly available.

Results

Patient demographics

Twenty patients were enrolled in "Part 1" and screened for eligibility. Nine did not meet criteria for enrollment for "Part 2." Between May 2017 and November 2020, 11 patients received nivolumab on study at a dose of 3 mg/kg every 2 weeks until confirmed disease progression, intolerable toxicity, or for a maximum of 24 months. Data cutoff for outcomes was March 2022. All patients had failed first-line therapies. Radiation was delivered >6 months prior to recurrence and trial enrollment for all patients receiving prior radiotherapy. Although the protocol allowed palliative radiation at least 14 days before trial commencement, none of the patients received (re)-irradiation prior to the initiation of nivolumab. Patients were eligible only after recovery of acute toxic effects of previous anticancer therapy (see trial protocol, Supplementary Appendix).

One individual withdrew consent from all aspects of the trial immediately following the first dose without any evidence of progression or toxicity. As per the trial mandate requiring completion of at least one cycle (two doses) for endpoint assessments, this patient was excluded from further follow-up and outcome analyses (**Fig. 1**). Median age of the final cohort ($n = 10$) was 14 years (range, 9–18; **Table 1**; Supplementary Table S1). Cancer diagnoses included malignant gliomas ($n = 7$; glioblastoma $n = 5$), neuroblastoma ($n = 1$), colorectal carcinoma ($n = 1$), and adrenocortical carcinoma ($n = 1$; ACC; **Fig. 2A**).

Baseline genomic characteristics and cancer predisposition

Three children had been enrolled on the basis of loss of MMR protein expression (all had TMB> 10 mut/Mb), six based on TMB >10 mut/Mb (five of whom also had IHC loss), while a single patient was enrolled for TMB of 7.4 mut/Mb with an MMR-proficient tumor (**Table 1**; **Fig. 2B** and **C**). Mutational signature (COSMIC; ref. 23) analyses demonstrated single-base substitution (SBS) signatures of MMRD in eight of 10 cancers and concomitant DNA polymerase proofreading deficiency signatures along with a pathogenic *POLE* somatic variant in three of these eight MMRD cancers. Germline cancer predisposition was detected in nine of 10 patients [CMMRD: $n = 2$; Lynch syndrome: $n = 5$; one patient each with *PALB2* variant and Li-Fraumeni syndrome (LFS); **Table 1**]. The single patient without

Figure 2.
Characteristics and outcomes of patients: **A,** Cancer types included in the final analysis cohort. **B,** IHC patterns of MMR deficiency highlighted using representative patients: complete loss of PMS2 expression in all cells in a patient with CMMRD (P6); loss of PMS2 in tumor cells with retention in normal cells in a patient with Lynch syndrome (P1) and focal loss of MSH6 in only a subset of tumor cells in a patient with therapy-associated MMRD (P8; magnification: 100X, inset 400X). **C,** Oncoplot summarizing clinical and genomic features. Patients are arranged by their tumor's total SNV per megabase (on a semilogarithmic scale). **D,** Waterfall plot summarizing radiological responses of target lesions (++: rapid enlargement and exact measurements at progression not available; x: Divergent responses including response at nontarget site; #: Pathologic complete response; *: delayed response). This demonstrates that while initial ORR was 20% (P4, P6), the iBOR was 50% (including P2, P3, and P7). **E,** Swimmer plot summarizing patient course. Each solid box denoted time while on trial protocol. Some patients had termination of their trial protocol treatment due to progression or toxicity but thereafter received nivolumab through compassionate or commercial access, the duration of which are shown as dashed boxes. **F,** Survival for entire cohort: OS (blue) and PFS (yellow). **G,** Survival for CNS tumors: OS (blue) and PFS (yellow). The PFS curves are based on prior-defined radiologic criteria in the trial protocol (iRANO/iRECIST) and did not include the delayed responses (i.e., iBOR).

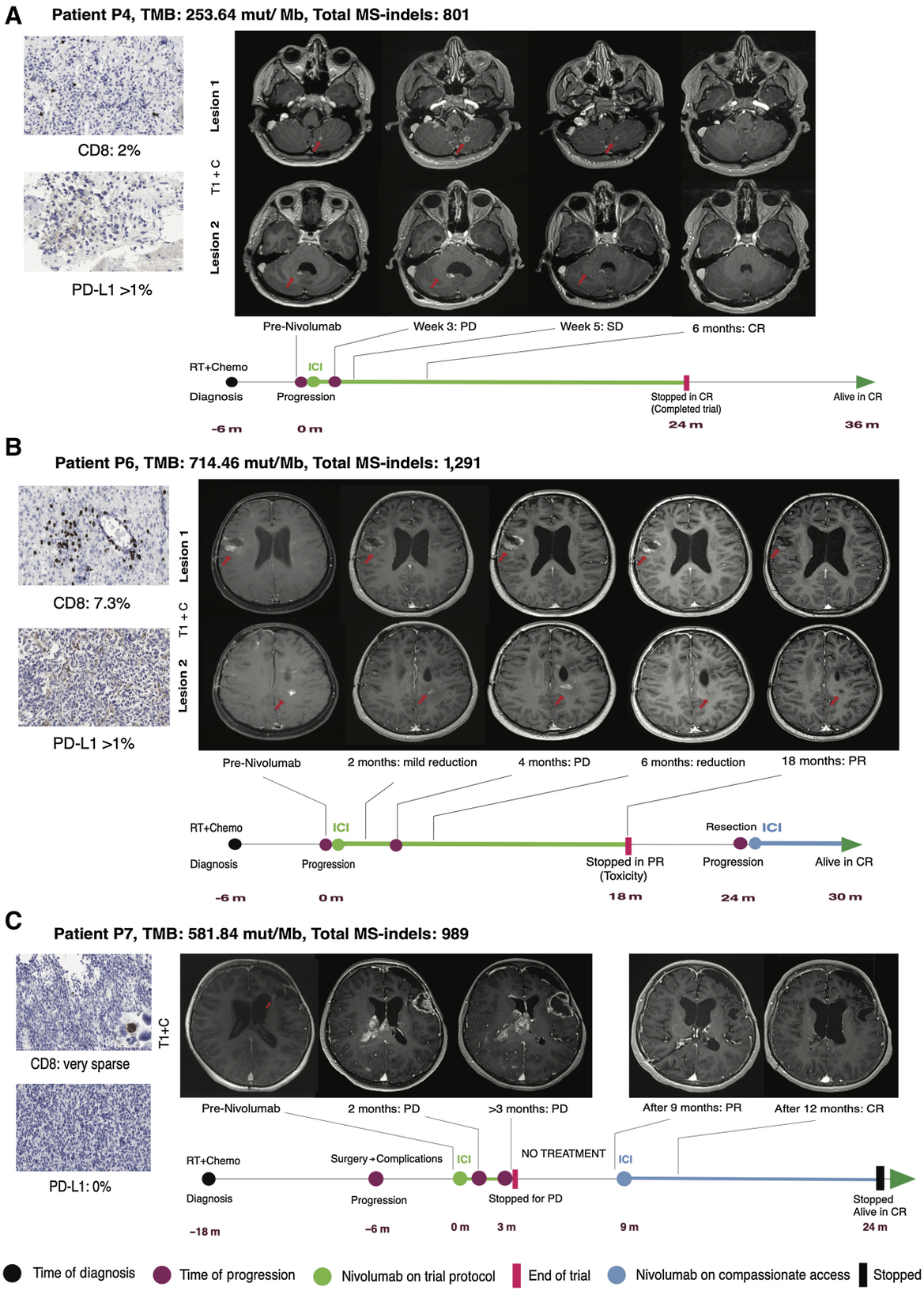
A
Patient P4, TMB: 253.64 mut/ Mb, Total MS-indels: 801
CD8: 2%
PD-L1 >1%
Lesion 1
T1 + C
Lesion 2
Pre-Nivolumab
Week 3: PD
Week 5: SD
6 months: CR
RT+Chemo
ICI
Diagnosis
Progression
Stopped in CR
(Completed trial)
Alive in CR
-6 m
0 m
24 m
36 m
B
Patient P6, TMB: 714.46 mut/Mb, Total MS-indels: 1,291
CD8: 7.3%
PD-L1 >1%
Lesion 1
T1 + C
Lesion 2
Pre-Nivolumab
2 months: mild reduction
4 months: PD
6 months: reduction
18 months: PR
RT+Chemo
ICI
Diagnosis
Progression
Stopped in PR
(Toxicity)
Resection
ICI
Progression
Alive in CR
-6 m
0 m
18 m
24 m
30 m
C
Patient P7, TMB: 581.84 mut/Mb, Total MS-indels: 989
CD8: very sparse
PD-L1: 0%
T1+C
Pre-Nivolumab
2 months: PD
>3 months: PD
After 9 months: PR
After 12 months: CR
RT+Chemo
Surgery+Complications
ICI
NO TREATMENT
ICI
Diagnosis
Progression
Stopped for PD
Stopped
Alive in CR
-18 m
-6 m
0 m
3 m
9 m
24 m
Time of diagnosis
Time of progression
Nivolumab on trial protocol
End of trial
Nivolumab on compassionate access
Stopped

germline predisposition (P8) had been previously treated with temozolomide, showed focal loss of staining for MSH6 in subpopulations of tumor cells suggesting subclonal MMR deficiency, and demonstrated signature 11 (23), suggesting that the MMR deficiency was acquired and driven by temozolomide treatment (**Fig. 2B**). None of the patients with germline MMR deficiency and high-grade gliomas had received temozolomide (37, 38).

Toxicity

Toxicity data were evaluated for all patients who received at least one dose of nivolumab and are summarized in **Table 2** ($n = 11$). Treatment was well tolerated. Seven patients experienced grade ≤2 treatment-related adverse events. The only significant autoimmune adverse event leading to treatment discontinuation was in a patient with glioblastoma (P6), who developed grade 3 pancreatitis (with grade 4 lipase elevation), after having previously experienced other immune-related side effects including grade 2 autoimmune gastritis and grade-1 noninfective cystitis. A second patient (P1) with glioma stopped following symptomatic hydrocephalus due to a rapid progression of a posterior fossa mass that subsequently needed to undergo debulking surgery.

Antitumor activity and patient survival

Disease status was evaluated every 2 months, and patients could continue therapy beyond iUPD, with subsequent scans being used to establish confirmed progression, or delayed "immune" responses, which could then be included in the best overall response (iBOR) even after discontinuation of protocol therapy (24, 25, 27, 28). Among 10 patients, nine had measurable disease, with evaluable-only disease in the patient with neuroblastoma. The initial radiological responses were complete response (CR) in one (P4), partial response (PR) in one (P6), SD in four, and PD in three patients (**Table 1**; **Fig. 2D**). Remarkably, delayed responses (iBOR) were observed in multiple patients even when the trial was terminated because of initial progression. This resulted in best overall responses to be reclassified as CR in three (P2, P4, P7), and PR in two patients (P6, P3; **Fig. 2D** and **E**). Hence, while the initial objective response rate was 20%, the best overall response was 50%. Recurrent tumors in patients who achieved iBOR exhibited significant to complete radiological regression (**Figs. 3** and **4**), and all who continued ICI treatment are alive at the time of reporting at a median follow-up of 37 months (range, 32.4–60) from trial enrollment. The best percentage change from baseline in target lesions is shown in **Fig. 2D**.

The median follow-up for the cohort was 20.8 months [95% confidence interval (CI), 11.2–30.4]. The median OS was 23.7 months (95% CI, 7.2–not reached), culminating in an estimated 2-year OS of 50% (95% CI, 27–93). The median PFS was 3.6 months (95% CI, 0.9–not reached), with an estimated 2-year PFS of 20% (95% CI, 6–69; **Fig. 2F**). For patients with malignant gliomas, the median OS was 16.2 months (95% CI, 7.2–not reached) with an estimated 2-year OS of 43% (95% CI, 18.2–100), while the median PFS was 2.7 months (95% CI, 0.9–not reached) with an estimated 2-year PFS of 14% (95% CI, 2.3–87.7; **Fig. 2G**). The delayed immune responses following initial progression contributed to the differences observed between PFS and OS, as only minority received additional nonimmune therapies after progression (**Table 1**).

Tumor genomic and immune biomarkers and neuroimaging response trajectories

On the basis of previous studies showing impact of tumoral genomic and immune biomarkers in determining outcome to ICI treatment (5, 29, 39–42), we investigated several biomarkers in responders and nonresponders at baseline (**Table 1**; **Fig. 2C**) and their spatiotemporal variability (**Figs. 3** and **4**; Supplementary Fig. S1) in select cases where repeat biopsies were performed. The unique trajectories to best overall responses in multiple patients in our trial in the context of these biomarkers revealed the following interesting observations.

An adolescent with Lynch syndrome and multifocal recurrent glioblastoma (P4), where the baseline tumor had elevated TMB, MSI, CD8 T-cell infiltration and PD-L1 expression (ref. 29; **Fig. 3A**; **Table 1**) developed initial tumor "flare" (ref. 29; pseudoprogression or iUPD; **Figs. 2E** and **3A**) at multiple sites after the second dose of nivolumab. Clinical deterioration mandated admission to the intensive care unit. Symptoms subsided with supportive management without any immunosuppressive (steroid) treatment. He continued on protocol treatment, achieved CR, and is alive 3 years following initiation of nivolumab and 1 year after completing the trial.

The second survivor (P6) with CMMRD and recurrent multifocal glioblastoma demonstrated initial radiological progression without worsening symptoms (iUPD; **Figs. 2E** and **3B**) and continued protocol therapy, eventually achieving PR prior to stopping the trial due to severe pancreatitis (**Fig. 2E**). This tumor also has extreme mutation and MSI burden, along with elevated CD8 and PD-L1 expression. After a local relapse 6 months after stopping protocol treatment due to severe toxicity, he was rechallenged with nivolumab (compassionate access) and remains in CR without toxicity recurrence at data cutoff.

A third survivor (P7) with CMMRD achieved delayed CR after sustained massive disease progression on serial imaging for 3 months on protocol treatment, prompting discontinuation of trial therapy (**Figs. 2E** and **3C**). Notably, the tumor at baseline had highly elevated TMB and MSI, but lacked CD8 and PD-L1 expression. Continued clinical improvement while at home on hospice care prompted an imaging more than 6 months after stopping therapy. Remarkably, even in the absence of any intervening therapy, this demonstrated PR. She

Figure 3.

Response after pseudoprogression and true progression following ICI treatment in three survivors with glioblastoma. **A,** Early "flare" on ICI treatment (P4). Two lesions in the posterior fossa at time of progression measured 6×6 mm (right) and 5×3 mm (left). On week 3, there was significant clinical deterioration needing intensive care, and MRI demonstrated increase to 9×9 mm and 8×9 mm, respectively. Supportive care without use of steroids led to clinical improvement and next MRI showed reduction to 6×5 mm and 6×4 mm, respectively. The patient continued on trial protocol and the 6-month scan confirmed CR. **B,** Early interim progression and response (P6). Multifocal disease, with two of the largest lesions measuring 10.5×9 mm (target lesion) and 9×8 mm at progression. After start of protocol, MRI at 3 months showed mild reduction in size to 10×8 mm and 9×7 mm, respectively. The next MRI showed progression, with increase to 18.6×11 mm and 14×8.2 mm, but the patient was stable. Continued treatment on protocol showed reduction to 10.7×6.8 mm and 9.6×7.5 mm, respectively at 6 months. Patient attained PR for target site, and the other sites of disease had disappeared completely when the trial had to be stopped because of severe pancreatitis. **C,** Delayed response after initial massive and sustained progression (P7). The target lesion at the primary surgical bed at start of protocol treatment was 6×5 mm, which continued to show significant progression continuously through months 2 (31×29 mm) and 3 (47×37 mm), along with metastatic progression at other sites, following which patient was shifted to palliative home care without any anticancer therapy or steroids. Clinical improvement after 9 months prompted MRI that showed reduction to 5×3 mm, the patient was restarted on nivolumab, achieved CR, and completed 24 months of treatment.

was restarted on nivolumab (compassionate access) and is alive in CR after completing 2 years of therapy. All three patients with aggressive CNS tumors also harbored a second, somatic *POLE* mutation in their tumors contributing to the ultra-hypermutation (TMB >100 mut/Mb; ref. 43) in their tumors.

The fourth survivor had Lynch syndrome and metastatic colorectal carcinoma (P2) with moderately elevated TMB but a very high MSI burden (**Table 1**). She demonstrated radiological SD, but pathologic CR was demonstrated when the residual lesion was resected and showed only inflammation with no detectable tumor cells (Supplementary Fig. S1). Furthermore, there was elevation of CD8 and PD-L1 expression in this second biopsy as compared with the primary specimen. She remains in remission for 60 months from enrollment (**Fig. 2E**).

Interestingly, two additional deceased patients with Lynch syndrome had mixed responses attributable to divergent TMB and/or tumor locations that deserve further elaboration. Sustained symptomatic progression in patient P3 following initial disease stability prompted a biopsy (**Fig. 4A**). An increase in TMB and MSI burden were noted. In addition, 83% of mutations in the second biopsy were novel and distinct from the primary specimen. There was also higher CD8 T-cell infiltration and PD-L1 expression as compared with baseline. The tumor continued to symptomatically progress following rechallenge of immunotherapy postsurgery, leading to midline shift and visual deterioration, and no further ICI treatment was administered thereafter. Remarkably, there was delayed PR 5 months later without further intervention. Ultimately, there was another progression after 12 months, which culminated in fatality approximately 16 months from trial enrollment.

Another patient with metastatic recurrence (P1) demonstrated progression of two of her lesions, including the primary target temporal glioma that had a moderately elevated TMB and high MSI burden (**Table 1**). On trial, a rapidly enlarging posterior fossa mass caused significant symptomatic hydrocephalus, requiring surgical debulking. This specimen did not have any CD8 or PD-L1 expression in contrast to the primary lesion. Furthermore, this posterior fossa lesion and the primary tumor had only 1% of mutations shared between them, suggesting that the two lesions were genomically disparate, plausibly with distinct neoantigen expression that resulted in different immune microenvironment characteristics. Though treatment was stopped culminating in rapid fatality, strikingly, a third lesion detected pretherapy that was never biopsied showed reduction in size with nivolumab treatment (**Fig. 4B**).

Overall, within this cohort of cancers with elevated TMB, we observed that children whose tumors harbored higher (≥median) total indel and MS indel burden had improved survival (median OS not reached for both; **Fig. 5A**). Association of CD8 and PD-L1 expression with response and survival were variable (**Fig. 2C**).

Immune biomarkers in peripheral blood

We performed exploratory immune cell subset analyses from serial blood samples collected at predetermined timepoints as indicated in the trial protocol that provided additional insights. First, responders, including patients who had delayed responses after sustained initial progression (P7, P3), had higher 4-1BB+ CD8 T cells in blood at baseline, as well as achieved a higher peak of these activated populations of T cells on immunotherapy (**Fig. 5B**). Nonresponders had higher regulatory T cells ($CD4^+$) in blood at baseline, and their nadir counts in serial measurements stayed higher than responders (**Fig. 5C**). Furthermore, patients with persistently elevated regulatory T cells after the first 3 months on trial had a higher risk of death (Supplementary Table S2). Finally, pilot analyses of serial peripheral blood TCR-beta (TRB) rearrangement were performed for three responders and three nonresponders over the first 3 months of treatment (44). The responders had a higher total clone count, as well as higher richness (measured by Shannon diversity) and evenness (measured by Gini coefficient) of clonal distribution than nonresponders (ref. 44; **Fig. 5D**).

Discussion

In this article, we present the first prospective clinical trial using nivolumab exclusively for children with refractory solid and brain tumors with high TMB. Best overall responses (50%) exceeded initial objective radiological response (20%), translating to ongoing prolonged ongoing survival in four of five responders with rapidly fatal cancers when continued on ICI treatment. Despite a premature termination for slow accrual and loss of funding, our trial, like select others (45), could still provide us with several important clinical and biological insights for this unique cohort of childhood cancers with elevated mutation load.

We noted that the high TMB in our cohort of refractory pediatric cancers had diverse etiologies, which plausibly had an impact on ICI response, as had also been recently proposed by an international multistakeholder group on ICI use in pediatric cancers (20). All five responders in this trial exhibited MMRD, which uniquely for our cohort of pediatric patients was predominantly of germline origin and related to well-characterized cancer predisposition syndromes. Cancers in the two children with constitutional (biallelic) MMRD demonstrated ultra-hypermutation (TMB > 100 mut/Mb) with concomitant DNA polymerase proofreading deficiency (43) and responded following ICI. Remarkably, we also witnessed responses among three of five patients with Lynch syndrome, where the cancers had both hypermutation and evidence of somatic MMRD as was demonstrated using IHC and mutational signature analysis [COSMIC SBS signatures 6, 15, 20 (31)]. It is likely that germline MMRD contributes to improved survival on immunotherapy because of the continuous obligatory mutation accumulation (43) leading to higher neoantigen expression. An additional important contributor could be the concomitant presence of high MS-indel burden (29), as frameshift mutations can generate "higher-quality" neoantigens, especially if the indels are in MS in coding loci (29, 46). It is important to note that for pediatric cancers, MSI panels developed for adults have low sensitivity and appropriate genomic assays should be incorporated for incorporation of MSI-high pediatric cancers in future ICI studies (33, 47).

In this context, it is important to highlight that the patient with GBM where MMRD was acquired following temozolomide treatment (P8) did not respond to nivolumab despite having a high TMB. As observed in adult glioblastomas that historically do not respond to ICI (7), this tumor harbored SBS 11 (7, 31) and had only limited focal areas of loss of MMR staining (**Fig. 2B**), suggesting subclonality for acquired MMRD, plausibly contributing to the low MSI burden and lack of ICI response (7, 29). Similarly, an elevated TMB arising from other etiologies was not associated with response to ICI. This included a patient with neuroblastoma (P5) with a defect in the homologous recombination repair (HRD) pathway harboring SBS 3 (HRD signature; ref. 31) and a patient with LFS and ACC (P10). Together, these data suggest that in children, hypermutation driven by germline MMRD is likely essential for ICI response.

The dynamic responses that we observed in several patients with germline MMRD-induced hypermutation are worth further discussion. While early tumor "flare" or pseudoprogression has been reported previously (ref. 29; P4; **Fig. 3A**), we witnessed clear sustained and symptomatic tumor progression on nivolumab prior

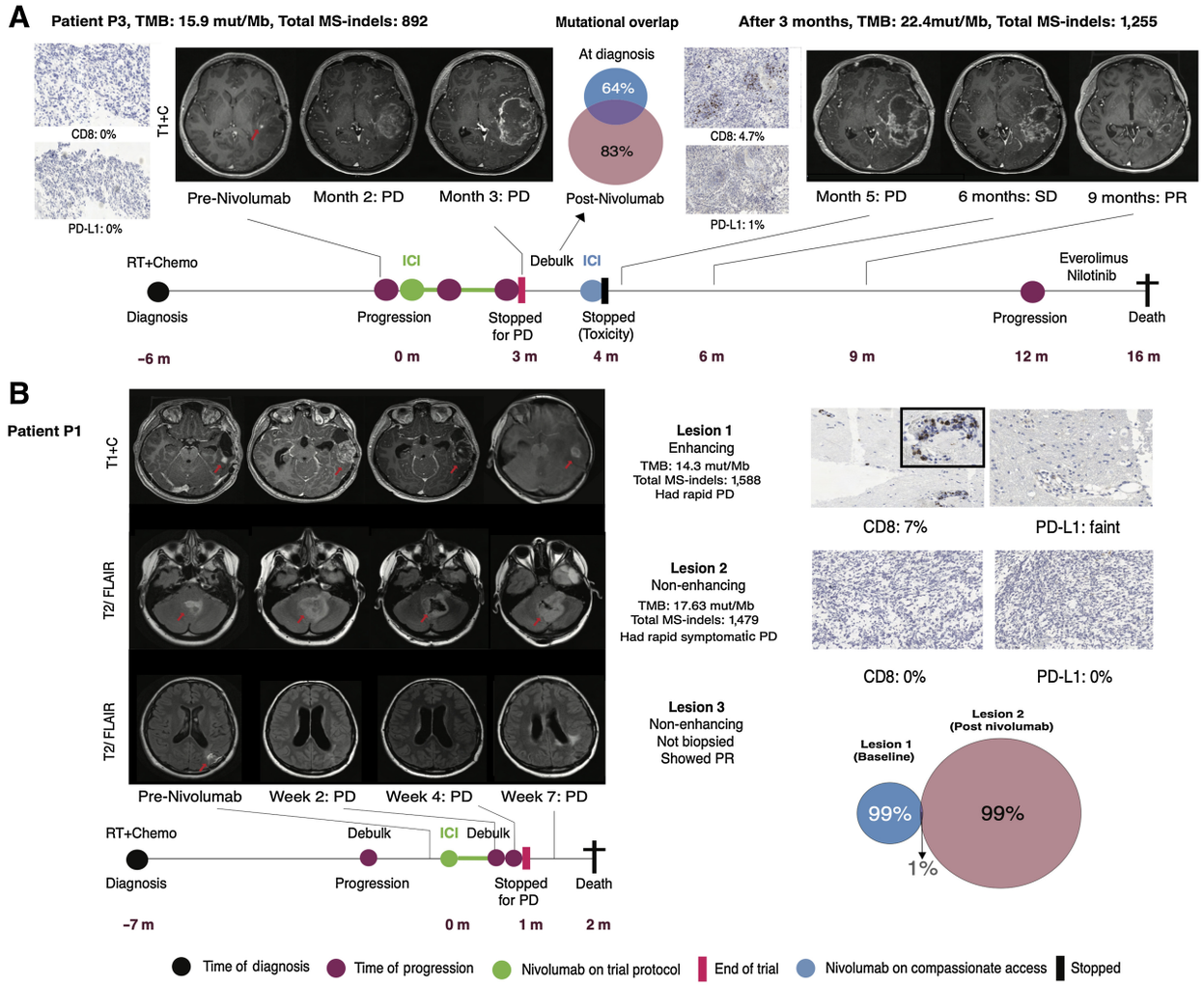

Figure 4.

Biological explanation for unique and divergent response trajectories for two deceased children with high-grade gliomas. **A,** Tumor evolution on ICI and impact on microenvironment (P3). At protocol initiation, the lesion was 55×45 mm, progressed to 66×45 mm after a month and 85×51 mm in the third month. Debulking was done and biopsy showed an increase in TMB and novel mutation accumulation, as shown using a Venn diagram depicting the overlap of variants at baseline (blue) and at the time of progression (dark pink). Simultaneously, there was an increase in CD8 and PD-L1 expression at the time of the second biopsy. The tumor progressed symptomatically to 90.5×62 mm after restarting ICI postsurgery, and treatment was stopped. Serial scans without further treatment showed stabilization and subsequently reduction to 38×30 mm, before further progression and death. All IHC images are 100X (inset: 400X). **B,** Divergent responses following ICI in biologically distinct lesions in the same patient (P1). Massive radiological progression in lesion 1 (from 10.9×8.8 mm to 47×29 mm), which was the target lesion along with rapid symptomatic progression in lesion 2 (from 28×23 mm to 53×48 mm) soon after trial initiation mandated debulking of lesion 2. Comparison of lesions 1 (biopsy at baseline) and 2 (after rapid progression on nivolumab) showed different TMB and MSI burden, with insignificant overlap of mutations as shown using a Venn diagram for the primary (blue) and posterior fossa (dark pink) lesions. This suggested that these were biologically distinct gliomas with very different immune microenvironments. Lesion 2 in the posterior fossa showed massive regrowth very rapidly after debulking. Lesion 3 (initially 16×15 mm) was never biopsied but showed radiological response on nivolumab treatment. All IHC images are 100X (inset: 400X).

to delayed responses and prolonged survival in three children (P3, P6, P7; **Figs. 3B** and **C** and **4A**). Such prolonged survival with continuation of ICI postprogression has been noted in adult cancers like melanoma (48). The patient with ultra-hypermutant MMRD glioblastoma (P7) had low CD8 expression at diagnosis and sustained progression for >3 months resulting in trial termination. Repeat scans 6 months without additional therapy demonstrated response, leading us to hypothesize that MMRD-driven genomic instability can contribute to stochastic mutation accumulation over time, conferring delayed immunogenicity (43). This was objectively demonstrated in another patient (P3), where a biopsy during progression showed that the glioma now harbored a higher TMB, leading to higher immunogenicity, as demonstrated by both higher CD8 and PD-L1 expression (29) in the tumor, plausibly contributing to the delayed response. Similar evidence of radiological progression for several weeks was also noted in patient P6 before delayed and sustained response, contributing to prolonged ongoing survival. Of note, among CNS tumors, responders with lower tumor burden (P4, P6) had a relatively earlier response than those with higher disease burden (P3, P7), where despite favorable genomic biomarkers, response was

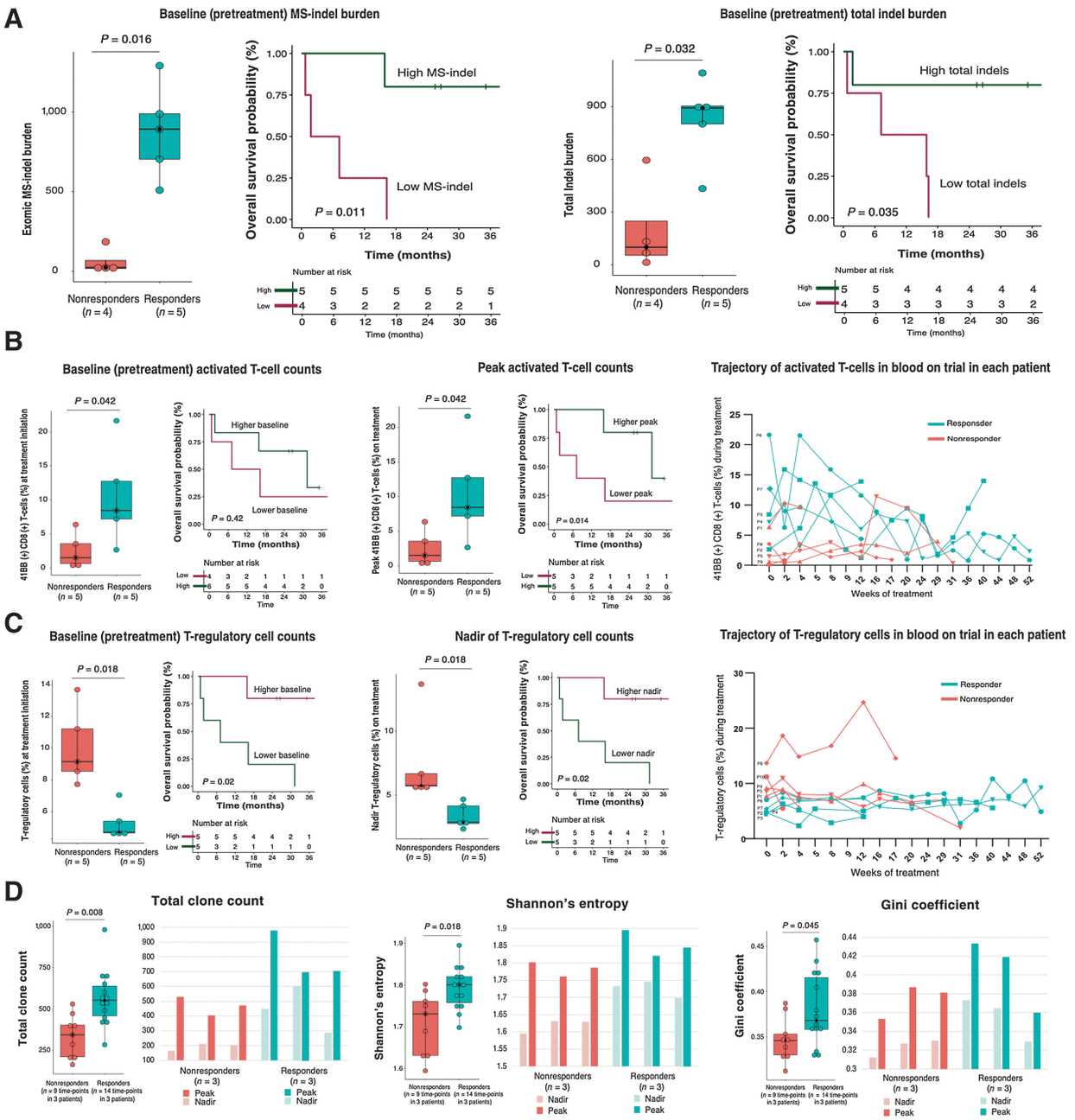

Figure 5.

Biomarker analyses. Tumor biomarker analyses. **A,** MS indel and total indel burden. Responders had higher levels of both MS and total indels and higher levels stratified OS probability. (Cutoff for high and low for Kaplan–Meier survival curves are medians for respective cohorts. Shaded portions signify 95% CI.) Peripheral blood. **B,** Activated T cells (4-1BB+ $CD8^+$ T cells as % of total T cells): At treatment initiation, peak, and trajectory during the first year. Responders had higher activated T cells at baseline and achieved higher peaks during ICI treatment. **C,** Regulatory T cells (%): At treatment initiation, nadir, and trajectory during the first year. Responders had lower regulatory T cells at baseline and lower nadir during ICI treatment. Both stratified OS probability. **D,** TRB clonotype analysis: clone count and diversity indices compared between responders and nonresponders, with peak and nadir measurements while on treatment.

delayed beyond 6 months (**Fig. 2E**). There is increasing evidence that a higher tumor burden negatively impacts the microenvironment and can modulate response to checkpoint inhibitors (49).

It is also important to note that we observed different lesions in the same patient, which are conventionally considered as metastatic tumors at relapse, could be biologically heterogeneous and consequently have different responses (P1; **Fig. 4B**). This could be attributed to random mutation accumulation secondary to MMRD in lesions at different sites. These findings highlight the challenges of conventional radiological assessments in children treated with immunotherapy and

combined with the delay in responses observed by us, may account for limited responses seen in some previous studies in children receiving ICI treatment.

Finally, although limited by the small numbers, continuous collection of biomarkers in the blood and in tumor tissue at progression in our trial provided us with additional biological insights. We did not find a reliable association between PD-L1 expression and patient outcome (**Fig. 2C**) plausibly linked to cancer-driven immune editing (50), as MMRD tumors in our trial exhibited change in PD-L1 expression over time (**Fig. 4A**; refs. 51, 52). Similarly, while we observed variable and consistent elevation of CD8 (+) T cells in the microenvironment plausibly driven by neoantigen expression caused by the high TMB, this too could change over time (**Fig. 4A** and **B**), confounding associations of baseline measurements on diagnostic biopsies with response at recurrence following ICI treatment.

Interestingly, serial peripheral blood analysis during treatment on trial did show important correlation between tumor response and immune activation. Activated 4-1BB+$CD8^+$ T cells, higher levels of which have been previously associated with antitumor immune responses (53, 54, 29), were uniformly and significantly elevated in all five responders in our study. Interestingly, patient P1, who demonstrated divergent responses at three sites including radiological response in one lesion, also had elevated activated 4-1BB+$CD8^+$ T-cell counts (**Fig. 5B**). This suggested that asymmetric and atypical responses could be potentially identified by peripheral biomarkers. We also found lower regulatory T cells in the peripheral blood of responders, as has been recently linked to more effective antitumor responses (55). In addition, we observed that responders had both higher richness and evenness of their TRB clonal repertoire. While we did observe increase in skewness (Gini coefficient) of the TRB repertoire over time, we did not find enrichment of specific TCR sequences (measured by reduction of Shannon entropy) as has been previously reported in responders following ICI treatment (56–60). This is plausibly related to the high, ongoing mutation accumulation and neoantigen expression in MMRD cancers that leads to a dominance of multiple TRB clones. These intriguing findings may be specific to germline MMRD where cancers arise in the backdrop of constitutional genomic instability that need to be evaluated in more detail in future studies.

In summary, our trial shows benefit of nivolumab treatment in pediatric patients with MMRD cancers with elevated TMB, including lethal malignant gliomas, with an acceptable safety profile. During ICI treatment, clinicians need to be aware of early pseudoprogression, differential responses at distinct sites, and delayed responses due to changing tumor immunogenicity. Future approaches could involve biomarker-driven front-line use in aggressive tumors like malignant ultra-hypermutant gliomas with favorable biomarkers (61, 62) and exploration of combinatorial approaches in patients failing anti-PD1 monotherapy (63). Routine use of MMR IHC, the incorporation of TMB and mutational signatures into cancer sequencing analyses, and screening patients from low and middle-income countries (64, 65) with a higher prevalence of germline MMRD can improve outcomes for these patients worldwide.

Authors' Disclosures

L.C. Sambira Nahum reports grants from BioCanRx Grant during the conduct of the study. S. Sudhaman reports other support from Natera Inc outside the submitted work. G. Getz reports personal fees from Scorpion Therapeutics during the conduct of the study; grants from Pharmacyclics outside the submitted work; has a patent for MSMutect pending, a patent for MSMutSig pending, and a patent for MSIDetect pending; and is an inventor on additional patent applications related to POLYSOLVER, SignatureAnalyzer-GPU, and MinimuMM-seq. Y.E. Maruvka reports grants from Israeli Science Foundation and grants from Israel Cancer Association during the conduct of the study and personal fees from ForeseeGenomics outside the submitted work. B. Ertl-Wagner reports personal fees from Bayer Healthcare outside the submitted work; and spouse is an employee of Siemens Healthineers. T. Pugh reports personal fees from AstraZeneca, Chrysalis Biomedical Advisors, Merck, and SAGA Diagnostics, and grants from Roche/Genentech outside the submitted work. C. Hawkins reports grants from CIHR, CCS, The Cure Starts Now, Meagan's Hug, and Genome Canada outside the submitted work; and has a patent for LOGIC pending. E. Bouffet reports grants from BMS during the conduct of the study and personal fees from Novartis and Alexion (AstraZeneca) outside the submitted work. D.A. Morgenstern reports grants from BMS during the conduct of the study; personal fees from ymAbs Therapeutics, Clarity Pharmaceuticals, Regeneron, and Rayzebio Inc, and other support from Abbvie and Oncoheroes Biosciences outside the submitted work. No disclosures were reported by the other authors.

Disclaimer

The funders had no role in the collection, analyses, or interpretation of data; in the writing of the article; or in the decision to publish the results.

Authors' Contributions

A. Das: Software, formal analysis, funding acquisition, validation, investigation, visualization, methodology, writing–original draft, writing–review and editing. **U. Tabori:** Conceptualization, resources, data curation, formal analysis, supervision, funding acquisition, investigation, methodology, writing–review and editing. **L.C. Sambira Nahum:** Resources, investigation, project administration. **N.B. Collins:** Conceptualization, resources, investigation, project administration. **R. Deyell:** Conceptualization, resources, investigation, project administration. **R. Dvir:** Resources, investigation. **C. Faure-Conter:** Resources, investigation. **T.E. Hassall:** Resources, investigation. **J.E. Minturn:** Resources, investigation. **M. Edwards:** Resources. **E. Brookes:** Resources. **V. Bianchi:** Resources. **A. Levine:** Investigation. **S.C. Stone:** Investigation, visualization. **S. Sudhaman:** Investigation, visualization. **S. Sanchez-Ramirez:** Investigation, visualization. **A.B. Ercan:** Investigation. **L. Stengs:** Resources. **J. Chung:** Investigation. **L. Negm:** Investigation. **G. Getz:** Software, investigation. **Y.E. Maruvka:** Software, validation. **B. Ertl-Wagner:** Formal analysis, investigation, visualization. **P.S. Ohashi:** Formal analysis, investigation, visualization. **T. Pugh:** Formal analysis, investigation, visualization. **C. Hawkins:** Formal analysis, investigation. **E. Bouffet:** Conceptualization, resources, formal analysis, supervision, funding acquisition, investigation, methodology, writing–review and editing. **D.A. Morgenstern:** Conceptualization, resources, data curation, formal analysis, supervision, funding acquisition, validation, investigation, visualization, methodology, writing–original draft, project administration, writing–review and editing.

Acknowledgments

The authors thank Aiman Siddiqi, Emily Taylor, Shaherose Nanji, Entela Zaffino, Nicole Sarvaria, and Alana Bougie at Hospital for Sick Children and the team at Ozmosis for assistance with trial management. Nivolumab and funding for the study and correlative biology were provided by BMS. A. Das would like to acknowledge the support of the St. Baldrick's Foundation International Scholar Award (with support from Kai Slockers Pediatric Cancer Research Fund), Stand Up to Cancer Maverick and Hold'em for Life awards. P.S. Ohashi would like to acknowledge the support from We Love You Conni Foundation.

The publication costs of this article were defrayed in part by the payment of publication fees. Therefore, and solely to indicate this fact, this article is hereby marked "advertisement" in accordance with 18 USC section 1734.

Note

Supplementary data for this article are available at Clinical Cancer Research Online (http://clincancerres.aacrjournals.org/).

Received February 9, 2023; revised March 23, 2023; accepted April 27, 2023; published first May 1, 2023.

References

1. Liu D, Schilling B, Liu D, Sucker A, Livingstone E, Jerby-Arnon L, et al. Integrative molecular and clinical modeling of clinical outcomes to PD1 blockade in patients with metastatic melanoma. Nat Med 2019;25:1916–27.
2. Garon EB, Rizvi NA, Hui R, Leighl N, Balmanoukian AS, Eder JP, et al. Pembrolizumab for the treatment of non-small-cell lung cancer. N Engl J Med 2015;372:2018–28.
3. Topalian SL, Hodi FS, Brahmer JR, Gettinger SN, Smith DC, McDermott DF, et al. Five-year survival and correlates among patients with advanced melanoma, renal cell carcinoma, or non-small cell lung cancer treated with nivolumab. JAMA Oncol 2019;5:1411–20.
4. Mandal R, Samstein RM, Lee K-W, Havel JJ, Wang H, Krishna C, et al. Genetic diversity of tumors with mismatch repair deficiency influences anti-PD-1 immunotherapy response. Science 2019;364:485–91.
5. Rousseau B, Foote MB, Maron SB, Diplas BH, Lu S, Argilés G, et al. The spectrum of benefit from checkpoint blockade in hypermutated tumors. N Engl J Med 2021;384:1168–70.
6. Notarangelo G, Spinelli JB, Perez EM, Baker GJ, Kurmi K, Elia I, et al. Oncometabolite d-2HG alters T cell metabolism to impair CD8(+) T cell function. Science 2022;377:1519–29.
7. Touat M, Li YY, Boynton AN, Spurr LF, Iorgulescu JB, Bohrson CL, et al. Mechanisms and therapeutic implications of hypermutation in gliomas. Nature 2020;580:517–23.
8. Sampson JH, Gunn MD, Fecci PE, Ashley DM. Brain immunology and immunotherapy in brain tumours. Nat Rev Cancer 2020;20:12–25.
9. Khasraw M, Reardon DA, Weller M, Sampson JH. PD-1 inhibitors: do they have a future in the treatment of glioblastoma? Clin Cancer Res 2020;26:5287–96.
10. Davis KL, Fox E, Merchant MS, Reid JM, Kudgus RA, Liu X, et al. Nivolumab in children and young adults with relapsed or refractory solid tumours or lymphoma (ADVL1412): a multicentre, open-label, single-arm, phase 1–2 trial. Lancet Oncol 2020;21:541–50.
11. Geoerger B, Kang HJ, Yalon-Oren M, Marshall LV, Vezina C, Pappo A, et al. Pembrolizumab in paediatric patients with advanced melanoma or a PD-L1-positive, advanced, relapsed, or refractory solid tumour or lymphoma (KEYNOTE-051): interim analysis of an open-label, single-arm, phase 1–2 trial. Lancet Oncol 2020;21:121–33.
12. Geoerger B, Zwaan CM, Marshall LV, Michon J, Bourdeaut F, Casanova M, et al. Atezolizumab for children and young adults with previously treated solid tumours, non-Hodgkin lymphoma, and Hodgkin lymphoma (iMATRIX): a multicentre phase 1–2 study. Lancet Oncol 2020;21:134–44.
13. Loeb DM, Lee JW, Morgenstern DA, Samson Y, Uyttebroeck A, Lyu CJ, et al. Avelumab in paediatric patients with refractory or relapsed solid tumours: dose-escalation results from an open-label, single-arm, phase 1/2 trial. Cancer Immunol Immunother 2022;71:2485–95.
14. Merchant MS, Wright M, Baird K, Wexler LH, Rodriguez-Galindo C, Bernstein D, et al. Phase I clinical trial of ipilimumab in pediatric patients with advanced solid tumors. Clin Cancer Res 2016;22:1364–70.
15. Haworth KB, Leddon JL, Chen CY, Horwitz EM, Mackall CL, Cripe TP. Going back to class I: MHC and immunotherapies for childhood cancer. Pediatr Blood Cancer 2015;62:571–6.
16. Simon AK, Hollander GA, McMichael A. Evolution of the immune system in humans from infancy to old age. Proc Biol Sci 2015;282:20143085.
17. Routy B, Le Chatelier E, Derosa L, Duong CPM, Alou MT, Daillère R, et al. Gut microbiome influences efficacy of PD-1-based immunotherapy against epithelial tumors. Science 2018;359:91–7.
18. Majzner RG, Simon JS, Grosso JF, Martinez D, Pawel BR, Santi M, et al. Assessment of programmed death-ligand 1 expression and tumor-associated immune cells in pediatric cancer tissues. Cancer 2017;123:3807–15.
19. Long AH, Morgenstern DA, Leruste A, Bourdeaut F, Davis KL. Checkpoint immunotherapy in pediatrics: here, gone, and back again. Am Soc Clin Oncol Educ Book 2022;42:1–14.
20. Pearson ADJ, Rossig C, Lesa G, Diede SJ, Weiner S, Anderson J, et al. ACCELERATE and European medicines agency paediatric strategy forum for medicinal product development of checkpoint inhibitors for use in combination therapy in paediatric patients. Eur J Cancer 2020;127:52–66.
21. Le DT, Uram JN, Wang H, Bartlett BR, Kemberling H, Eyring AD, et al. PD-1 blockade in tumors with mismatch-repair deficiency. N Eng J Med 2015;372:2509–20.
22. Campbell BB, Light N, Fabrizio D, Zatzman M, Fuligni F, de Borja R, et al. Comprehensive analysis of hypermutation in human cancer. Cell 2017;171:1042–56.
23. Alexandrov LB, Nik-Zainal S, Wedge DC, Aparicio SAJR, Behjati S, Biankin AV, et al. Signatures of mutational processes in human cancer. Nature 2013;500:415–21.
24. Seymour L, Bogaerts J, Perrone A, Ford R, Schwartz LH, Mandrekar S, et al. iRECIST: guidelines for response criteria for use in trials testing immunotherapeutics. Lancet Oncol 2017;18:e143–52.
25. Park JR, Bagatell R, Cohn SL, Pearson AD, Villablanca JG, Berthold F, et al. Revisions to the international neuroblastoma response criteria: a consensus statement from the national cancer institute clinical trials planning meeting. J Clin Oncol 2017;35:2580–7.
26. Ellingson BM, Huang RY-K, Villanueva-Meyer J, Lim-Fat MJ, George E, Iorgulescu B, et al. Estimated clinical efficacy and radiographic response characteristics of PD1 inhibition in newly diagnosed and recurrent glioblastoma in clinical practice: a report from the iRANO working group. J Clin Oncol 38: 15s, 2020 (suppl; abstr 2521).
27. Okada H, Weller M, Huang R, Finocchiaro G, Gilbert MR, Wick W, et al. Immunotherapy response assessment in neuro-oncology: a report of the RANO working group. Lancet Oncol 2015;16:e534–42.
28. Ellingson BM, Chung C, Pope WB, Boxerman JL, Kaufmann TJ. Pseudoprogression, radionecrosis, inflammation or true tumor progression? Challenges associated with glioblastoma response assessment in an evolving therapeutic landscape. J Neurooncol 2017;134:495–504.
29. Das A, Sudhaman S, Morgenstern D, Coblentz A, Chung J, Stone SC, et al. Genomic predictors of response to PD-1 inhibition in children with germline DNA replication repair deficiency. Nat Med 2022;28:125–35.
30. Rosenthal R, McGranahan N, Herrero J, Taylor BS, Swanton C. DeconstructSigs: delineating mutational processes in single tumors distinguishes DNA repair deficiencies and patterns of carcinoma evolution. Genome Biol 2016;17:31.
31. Alexandrov LB, Kim J, Haradhvala NJ, Huang MN, Tian Ng AW, Wu Y, et al. The repertoire of mutational signatures in human cancer. Nature 2020;578:94–101.
32. Maruvka YE, Mouw KW, Karlic R, Parasuraman P, Kamburov A, Polak P, et al. Analysis of somatic microsatellite indels identifies driver events in human tumors. Nat Biotechnol 2017;35:951–9.
33. Chung J, Maruvka YE, Sudhaman S, Kelly J, Haradhvala NJ, Bianchi V, et al. DNA polymerase and mismatch repair exert distinct microsatellite instability signatures in normal and malignant human cells. Cancer Discov 2021;11:1176–91.
34. Mulder DT, Mahé ER, Dowar M, Hanna Y, Li T, Nguyen LT, et al. CapTCR-seq: hybrid capture for T-cell receptor repertoire profiling. Blood Adv 2018;2:3506–14.
35. Benjamini Y, Hochberg Y. Controlling the false discovery rate: a practical and powerful approach to multiple testing. J R Statist Soc B 1995;57:289–300.
36. Benjamini Y, Cohen R. Weighted false discovery rate controlling procedures for clinical trials. Biostatistics 2017;18:91–104.
37. Tabori U, Hansford JR, Achatz MI, Kratz CP, Plon SE, Frebourg T, et al. Clinical management and tumor surveillance recommendations of inherited mismatch repair deficiency in childhood. Clin Cancer Res 2017;23:e32–7.
38. Liu L, Markowitz S, Gerson SL. Mismatch repair mutations override alkyltransferase in conferring resistance to temozolomide but not to 1,3-bis(2-chloroethyl) nitrosourea. Cancer Res 1996;56:5375–9.
39. Marabelle A, Fakih M, Lopez J, Shah M, Shapira-Frommer R, Nakagawa K, et al. Association of tumour mutational burden with outcomes in patients with advanced solid tumours treated with pembrolizumab: prospective biomarker analysis of the multicohort, open-label, phase 2 KEYNOTE-158 study. Lancet Oncol 2020;21:1353–65.
40. Le DT, Kim TW, Van Cutsem E, Geva R, Jäger D, Hara H, et al. Phase II open-label study of pembrolizumab in treatment-refractory, microsatellite instability-high/mismatch repair-deficient metastatic colorectal cancer: KEYNOTE-164. J Clin Oncol 2020;38:11–9.
41. Blank CU, Haanen JB, Ribas A, Schumacher TN. Cancer immunology. The "cancer immunogram." Science 2016;352:658–60.
42. Bai R, Lv Z, Xu D, Cui J. Predictive biomarkers for cancer immunotherapy with immune checkpoint inhibitors. Biomark Res 2020;8:34.
43. Shlien A, Campbell BB, de Borja R, Alexandrov LB, Merico D, Wedge D, et al. Combined hereditary and somatic mutations of replication error repair genes result in rapid onset of ultra-hypermutated cancers. Nat Genet 2015;47:257–62.

44. Chiffelle J, Genolet R, Perez MA, Coukos G, Zoete V, Harari A. T-cell repertoire analysis and metrics of diversity and clonality. Curr Opin Biotechnol 2020;65: 284–95.
45. Morgan CJ. Statistical issues associated with terminating a clinical trial due to slow enrollment. J Nucl Cardiol 2017;24:525–6.
46. Roudko V, Bozkus CC, Orfanelli T, McClain CB, Carr C, O'Donnell T, et al. Shared Immunogenic poly-epitope frameshift mutations in microsatellite unstable tumors. Cell 2020;183:1634–49.
47. Chung J, Negm L, Bianchi V, Stengs L, Das A, Liu ZA, et al. Genomic microsatellite signatures identify germline mismatch repair deficiency and risk of cancer onset. J Clin Oncol 2023;41:766–77.
48. Beaver JA, Hazarika M, Mulkey F, Mushti S, Chen H, He K, et al. Patients with melanoma treated with an anti-PD-1 antibody beyond RECIST progression: a US Food and Drug Administration pooled analysis. Lancet Oncol 2018;19:229–39.
49. Dall'Olio FG, Marabelle A, Caramella C, Garcia C, Aldea M, Chaput N, et al. Tumour burden and efficacy of immune-checkpoint inhibitors. Nat Rev Clin Oncol 2022;19:75–90.
50. Yi M, Niu M, Xu L, Luo S, Wu K. Regulation of PD-L1 expression in the tumor microenvironment. J Hematol Oncol 2021;14:10.
51. Xue W, Li W, Zhang T, Li Z, Wang Y, Qiu Y, et al. Anti-PD1 up-regulates PD-L1 expression and inhibits T-cell lymphoma progression: possible involvement of an IFN-gamma-associated JAK-STAT pathway. Onco Targets Ther 2019;12: 2079–88.
52. Takahashi T, Tateishi A, Bychkov A, Fukuoka J. Remarkable alteration of PD-L1 expression after immune checkpoint therapy in patients with non-small-cell lung cancer: two autopsy case reports. Int J Mol Sci 2019;20: 2578.
53. Ugolini A, Nuti M. CD137(+) T-cells: protagonists of the immunotherapy revolution. Cancers 2021;13:456.
54. Clouthier DL, Lien SC, Yang SYC, Nguyen LT, Manem VSK, Gray D, et al. An interim report on the investigator-initiated phase 2 study of pembrolizumab immunological response evaluation (INSPIRE). J Immunother Cancer 2019; 7:72.
55. Yoshida K, Okamoto M, Sasaki J, Kuroda C, Ishida H, Ueda K, et al. Anti-PD-1 antibody decreases tumour-infiltrating regulatory T cells. BMC Cancer 2020;20:25.
56. Poran A, Scherer J, Bushway ME, Besada R, Balogh KN, Wanamaker A, et al. Combined TCR repertoire profiles and blood cell phenotypes predict melanoma patient response to personalized neoantigen therapy plus anti-PD-1. Cell Rep Med 2020;1:100141.
57. Ott PA, Hu-Lieskovan S, Chmielowski B, Govindan R, Naing A, Bhardwaj N, et al. A phase Ib trial of personalized neoantigen therapy plus anti-PD-1 in patients with advanced melanoma, non-small cell lung cancer, or bladder cancer. Cell 2020;183:347–62.
58. Kato T, Kiyotani K, Tomiyama E, Koh Y, Matsushita M, Hayashi Y, et al. Peripheral T cell receptor repertoire features predict durable responses to anti-PD-1 inhibitor monotherapy in advanced renal cell carcinoma. Oncoimmunology 2021;10:1862948.
59. Postow MA, Manuel M, Wong P, Yuan J, Dong Z, Liu C, et al. Peripheral T cell receptor diversity is associated with clinical outcomes following ipilimumab treatment in metastatic melanoma. J Immunother Cancer 2015;3:23.
60. Han J, Duan J, Bai H, Wang Y, Wan R, Wang X, et al. TCR repertoire diversity of peripheral PD-1(+)CD8(+) T cells predicts clinical outcomes after immunotherapy in patients with non-small cell lung cancer. Cancer Immunol Res 2020;8: 146–54.
61. Larkin T, Das A, Bianchi V, Sudhaman S, Chung J, Alsafwani N, et al. Upfront adjuvant immunotherapy of replication repair–deficient pediatric glioblastoma with chemoradiation-sparing approach. JCO Precis Oncol 2021;5:1426–31.
62. Rittberg R, Harlos C, Rothenmund H, Das A, Tabori U, Sinha N, et al. Immune checkpoint inhibition as primary adjuvant therapy for an IDH1-mutant anaplastic astrocytoma in a patient with CMMRD: a case report-usage of immune checkpoint inhibition in CMMRD. Curr Oncol 2021;28:757–66.
63. Campbell BB, Galati MA, Stone SC, Riemenschneider AN, Edwards M, Sudhaman S, et al. Mutations in the RAS/MAPK pathway drive replication repair deficient hypermutated tumors and confer sensitivity to MEK inhibition. Cancer Discov 2021;11:1454–67.
64. Amayiri N, Tabori U, Campbell B, Bakry D, Aronson M, Durno C, et al. High frequency of mismatch repair deficiency among pediatric high grade gliomas in Jordan. Int J Cancer 2016;138:380–5.
65. Alphones S, Chatterjee U, Singh A, Das A, Zameer L, Achari R, et al. Immunohistochemical screening for mismatch repair protein deficiency in paediatric high-grade gliomas - institutional experience and review of literature. Childs Nerv Syst 2021;37:2521–30.